# MIXTURE-OF-EXPERTS CAN SURPASS DENSE LLMS UNDER STRICTLY EQUAL RESOURCE

## **Anonymous authors**

Paper under double-blind review

## **ABSTRACT**

Mixture-of-Experts (MoE) language models dramatically expand model capacity and achieve remarkable performance without increasing per-token compute. However, can MoEs surpass dense architectures under strictly equal resource constraints - that is, when the total parameter count, training compute, and data budget are identical? This question remains under-explored despite its significant practical value and potential. In this paper, we propose a novel perspective and methodological framework to study this question thoroughly. First, we comprehensively investigate the architecture of MoEs and achieve an optimal model design that maximizes the performance. Based on this, we subsequently find that an MoE model with activation rate in an optimal region is able to outperform its dense counterpart under the same total parameter, training compute and data resource. More importantly, this optimal region remains consistent across different model sizes. Although additional amount of data turns out to be a trade-off for enhanced performance, we show that this can be resolved via reusing data. We validate our findings through extensive experiments, training nearly 200 language models at 2B scale and over 50 at 7B scale, cumulatively processing 50 trillion tokens. All code and models will be released publicly.

## 1 Introduction

In recent years, Large Language Models (LLMs) based on the Transformer architecture (Vaswani, 2017) have achieved impressive results on a broad range of NLP tasks (Radford, 2018; Achiam et al., 2023; Touvron et al., 2023a;b; Bai et al., 2023). Meanwhile, there has been growing interest in using Mixture-of-Experts (MoE) layers (Shazeer et al., 2017) to expand model capacity while keeping the training cost reasonable (Fedus et al., 2022; Zoph et al., 2022; Rajbhandari et al., 2022). Recent open-source initiatives have explored MoE-based LLMs (Dai et al., 2024; Jiang et al., 2024; Wei et al., 2024; Xue et al., 2024; DeepSeek-AI et al., 2024b), yet many widely adopted open-source models such as LLaMA (Touvron et al., 2023a;b), DeepSeek's first-generation models (DeepSeek-AI et al., 2024a), and Qwen (Yang et al., 2024; Qwen et al., 2025), continue to utilize dense architectures, posing an open question of whether MoE LLMs can outperform their dense counterparts.

Current comparisons of MoE and dense LLMs often simplify the analysis to either a *data-centric* or a *compute-centric* perspective. The data-centric view, which keeps total training tokens constant for both MoE and dense models, praises MoE for its reduced activated parameter count per token (i.e., pertoken compute cost) and potential for aggressive parameter scaling. For example, DeepSeekMoE (Dai et al., 2024) reports a 16B-parameter MoE model (with 2.5B activated parameters) that achieves performance on par with a 7B dense model under the same data budget, thus suggesting a 2.5× "parameter-efficiency" advantage. The compute-centric view, which fixes total training compute, examines the impact of MoE sparsity (*i.e.*, the ratio of activated to total parameters) on performance. Under certain sparse configurations, total parameters can swell to nearly 100× those of a dense baseline, but at the cost of requiring more training data and managing high memory overhead.

However, neither perspectives fully addresses the complex interplay of critical resource constraints in large-scale model development: the finite nature of **training data volume** (D), **training compute** (C), and **model size** (N), which affects both memory and inference throughput. In particular, MoE models typically encounter bandwidth bottlenecks during inference, as all experts reside in GPU high-bandwidth memory and must be moved into shared memory, making parameter count a key

runtime cost factor beyond FLOPs. These interdependencies complicate the conclusion of the absolute superiority of MoE or dense architectures. Intuitively, a dense model with equivalent total parameters should have an advantage by fully utilizing its capacity. This often leads studies to favor MoE for scaling model size rather than direct comparisons at the same parameter count, thus overlooking the real-world resource constraints in large-scale training and deployment.

In this work, we introduce a novel perspective aimed at providing a more convincing resolution to this debate by posing the following question:

Can Mixture-of-Experts surpass dense LLMs under equal total parameter, compute, and data constraints?

To reach a definitive conclusion on this issue, we draw insights from a unified parameterization framework for model architecture ( $\S$  3) and propose a three-step experimental methodology. *First*, we search for an optimized architecture design to ensure each model candidate achieves its (near) optimal performance ( $\S$  4). *Second*, we explore the optimal activation rate based on this optimized model architecture, with the total parameters N and compute budget C fixed ( $\S$  5). *Third*, we present a data reuse strategy to address the additional data demand of MoE models, thereby equating data resource D ( $\S$  6). We also analyze the efficacy of this framework on downstream tasks ( $\S$  7).

Our findings, derived from extensive experiments and systematic evaluation under the proposed strict N/C/D parity with dense models, provide strong evidence that MoE architectures with optimized backbones and activation rates can indeed achieve superior performance over dense models on both upstream and downstream tasks. This implies that any observed performance gains can be attributed solely to architectural advantages, rather than disparities in parameter count or compute budget. Moreover, this challenges conventional wisdom and paves the way for resource-efficient yet powerful architectures in the next generation of large-scale NLP systems.

Our main contributions are: 1) We demonstrate, for the first time, that under fixed total parameters (N) and a fixed compute budget (C), an MoE LLM can surpass its dense counterpart with careful architecture design (see Fig. 1b, 2b). 2) Our experiments reveal the existence of a stable "optimal AR" region that consistently maximizes performance across varying N (see Fig. 1, 2). 3) We introduce a practical data reuse strategy that offsets MoE's additional data needs, enabling robust gains over dense models without substantially increasing unique training data D (see Fig. 2, 3).

## 2 Related Work

#### 2.1 MOE LANGUAGE MODELS

Building upon MoE (Shazeer et al., 2017), GShard (Lepikhin et al., 2020) facilitates model parallelism across devices for massive MoE models. With the advent of Transformers (Vaswani, 2017), the integration of MoE into the Transformer framework has become a popular model architecture and achieved state-of-the-art performance. As an early attempt, Switch Transformer (Fedus et al., 2022) proposes top-1 gating to simplify MoE architecture and alleviate communication overhead. More recent Transformer-based MoE LLMs include (Xue et al., 2024; Jiang et al., 2024; Wu et al., 2024; Wei et al., 2024; DeepSeek-AI et al., 2024b). The MoE architecture is briefly reviewed in Appendix A.

#### 2.2 Analyses of Moe Sparsity

Several studies investigated the impact of varying the number of MoE experts and adjusting granularity, both of which are factors related to sparsity. Through ablation studies, DeepSeekMoE (Dai et al., 2024) observes finer granularity results in improvement on overall model performance, and acquires a ratio between shared and routed experts that yields slightly better Pile loss. Zoph et al. (2022) summarized the results of several MoE works and indicated that the gain of increasing sparsity quickly diminishes when the number of experts is greater than 256 — a very sparse model.

Concurrently with our work, Ludziejewski et al. (2025) found that a sufficiently large MoEs trained with more tokens outperforms a dense model with the same total parameters. We further show MoE superiority even at smaller sizes and address the additional data demand via reuse. Abnar et al. (2025) studied the scaling law for optimal MoE sparsity. However, their models (up to  $N=30\mathrm{B}$ )

Table 1: Notation.

Symbol	Definition	Symbol	Definition
$\overline{D}$	Dataset size in tokens.	$\overline{S}$	Sequence length.
M	Compute (w/o embedding) per token in FLOPs.	H	Number of attention heads.
C	Total training compute in FLOPs, <i>i.e.</i> , $M \cdot D$ .	$D_{ m m}$	Model hidden dimension.
N	Number of non-vocabulary parameters.	$D_{ m ffn}$	FFN hidden dimension.
$N_{ m a}$	Number of activated parameters.	$D_{h}$	Dimension of attention head.
$r_{ m a}$	Activation rate, i.e., $N_a/N$ .	$D_{e}$	Expert hidden dimension.
$L_{ m e}$	Number of MoE layers.	$D_{se}$	Shared expert hidden dimension.
$L_{d}$	Number of dense layers.	E	Number of experts.
L	Number of total layers, i.e., $L_e + L_d$ .	K	Number of chosen experts.

were trained with  $C=1\mathrm{e}20$ , a much smaller budget compared to the approximately  $9\times$  and  $30\times$  compute we used for our 2B and 7B models to ensure an adequate D/N. This likely resulted in undertrained models, potentially affecting their conclusions. Moreover, our study first optimizes the MoE architecture to isolate the effect of different activation rates on performance. Detailed differences between our work and this previous study are discussed in Appendix B.

## 3 EXPERIMENTAL METHODOLOGY

We begin by introducing a unified parameterization framework for model architecture, establishing a solid foundation. Then, we derive key insights from this parameterization, which informs our comprehensive three-step experimental methodology. Finally, we detail the experimental setup used consistently across all subsequent experiments. Our notation is summarized in Table 1.

#### 3.1 Architecture Parameterization

To enable a comprehensive and general comparison of dense and MoE-based LLM architectures under realistic deployment constraints, we introduce a unified parameterization framework that explicitly accounts for both model parameters and per-token compute cost.

**Dense model parameterization.** For a dense model, we approximate the number of non-embedding parameters N and the per-token forward-pass computation cost M as follows:

$$N \approx (4+3\alpha)D_{\rm m}^2 L = (4+3\alpha)\zeta^2 L^3,$$
 (1)

$$M \approx 2N + 4D_{\rm m}SL = 2N + 4\zeta^2 \gamma L^3 \tag{2}$$

$$=2N(1+\frac{2\gamma}{(4+3\alpha)}),$$
 (3)

where  $\alpha = {}^{D_{\rm ffn}}/D_{\rm m}, \gamma = {}^{S}/D_{\rm m}$ , and  $\zeta = {}^{D_{\rm m}}/L$ . Here, we omit the LayerNorm parameter count as it is negligible. Inference cost or training cost can be approximated by  $C \approx M \times D$  or  $C \approx 3M \times D$ , respectively (based on the standard empirical observation that training typically takes about three times the forward pass for backward computation).

**MoE model parameterization.** In many real-world settings, only a subset of Transformer layers are replaced with MoE layers. The approximations for total non-vocabulary parameters N, activated parameters  $N_{\rm a}$ , and per-token computation cost M can be expressed as

$$N \approx (4+3\mu)D_{\rm m}^2 L_{\rm e} + (4+3\alpha)D_{\rm m}^2 L_{\rm d},$$
 (4)

$$N_{\rm a} \approx (4+3\beta)D_{\rm m}^2 L_{\rm e} + (4+3\alpha)D_{\rm m}^2 L_{\rm d},$$
 (5)

$$M \approx N_{\rm a} + 4D_{\rm m}SL = 2r_{\rm a}N + 4\zeta^2\gamma L^3,\tag{6}$$

where  $\mu = (D_{\text{se}} + ED_{\text{e}})/D_{\text{m}}$  and  $\beta = (D_{\text{se}} + KD_{\text{e}})/D_{\text{m}}$ . We again omit the parameters and FLOPs of the gating network (router) as they are comparatively small, and the *activation rate* (AR) is denoted as  $r_a$ . For the simple and common case where *all* L layers are MoE layers (*i.e.*,  $L_d = 0$ ), we have

$$r_{\rm a} = N_{\rm a}/N = (4+3\beta)/(4+3\mu),$$
 (7)

$$M \approx 2r_{\rm a}N + 4\zeta^2\gamma L^3 \tag{8}$$

$$=2r_{a}N(1+2\gamma/(4+3\beta)). \tag{9}$$

## 3.2 KEY OBSERVATIONS AND METHODOLOGICAL CONSIDERATIONS

Based on the above parameterization, we highlight the following insights that guide our experiments:

High structural degrees of freedom in MoE. Compared to a dense model (whose shape is almost uniquely determined by L,  $D_{\rm m}$ , and  $\alpha$ ), an MoE model has many more design choices: the number of MoE layers ( $L_{\rm e}$ ), expert-related dimensions (e.g., K, E,  $D_{\rm e}$ ,  $D_{\rm se}$ ), and so forth. Even with  $L_{\rm d}=0$ , the final shape depends on  $\mu$  and  $\beta$  in addition to  $\zeta$  and  $r_{\rm a}$ . Exhaustively searching all combinations is prohibitively expensive. Therefore, a greedy strategy should be adopted.

Activation rate  $r_a$  is the primary factor. At the same total parameter count N, the ratio of pertoken FLOPs between an MoE model and a dense model is primarily determined by the activation rate  $r_a$ . More specifically, if  $M_d$  is the per-token cost of the dense baseline (with  $\zeta$ ,  $\alpha$  fixed), then the pure MoE model's compute, normalized by  $M_d$ , roughly behaves as (the union of Equ. 3 and 9):

$$R_{\rm c} = r_{\rm a} \left( \frac{4 + 3\alpha + 2\gamma_{\rm d}}{4 + 3\beta + 2\gamma_{\rm m}} \right) \tag{10}$$

where  $\gamma_d$  and  $\gamma_m$  denote  $S/D_m$  for dense and MoE layers, respectively. As  $\gamma$  strongly correlates with  $\zeta$ , once the shape hyperparameters  $(\zeta, \alpha, \beta)$  are chosen,  $R_c$  grows monotonically with  $r_a$ .

The trade-off among N, C, and D. Once N (the total parameters) is chosen and we fix near-optimal shapes for dense and MoE models, the total training compute for the MoE model can be approximated by  $C=3\,R_{\rm c}\,M_{\rm d}\,D$ , where  $M_{\rm d}$  is the per-token cost of the dense baseline with the same total parameter count, and  $R_{\rm c}$  is the fraction by which the MoE model reduces compute per token (relative to the dense baseline). If we want to keep the same total compute C for both MoE and dense models, the MoE model will need  $R_{\rm c}$  times more training tokens.

#### 3.3 THREE-STEP EXPERIMENTAL METHODOLOGY

Motivated by the aforementioned observations, we propose a three-step experimental methodology which is both comprehensive and fair, so as to achieve the **new perspective** motivated in § 1 that enables a more conclusive comparison of MoE and dense LLMs under equal resource constraints. The methodology is outlined as follows: 1) **Greedy architecture determination.** First, decide the MoE to dense layer ratio ( $L_{\rm e}$  vs.  $L_{\rm d}$ ) to focus on MoE's internal benefits. Second, determine FFN parameter allocation (e.g., top-K) within each MoE layer. These are orthogonal to shape hyperparameters. Finally, choose the optimal shape hyperparameters ( $\zeta$ ,  $\beta$ ) for the MoE model. 2) **Activation rate analysis under fixed** N **and** C. With the optimal MoE architecture chosen in the previous step, and the optimal dense LLM shape proposed by Kaplan et al. (2020), we compare MoE models versus a dense baseline of the same size, ensuring the total training compute C is matched. Since C must be the same, the MoE model typically receives up to  $R_{\rm c}$  times more tokens (initially considering repeated or augmented data). 3) **Data reuse strategy.** To ensure a *truly* fair comparison at the same *unique* data budget D, we develop a data reuse strategy that offsets MoE's additional data requirement. This enables evaluation under strictly equal N, C, and D.

#### 3.4 COMMON EXPERIMENTAL SETUP

**Optimal hyperparameters.** MoE training is sensitive to the learning rate  $(\eta)$  and batch size (B) (He et al., 2024). Even minor architectural changes, such as variations in E, can lead to different optimal hyperparameters. To address this, we train all our models using the optimal  $\eta$  and B based on the hyperparameter scaling laws proposed in (Li et al., 2025). Specifically, Li et al. (2025) found that the optimal  $\eta$  and B follow power laws and depend only on N and D. Since these scaling laws are applicable to both dense and MoE models and are robust across various pretraining data distributions, we apply them to determining  $\eta$  and B for each of our experiments.

**Others.** We use internal, high-quality training and validation datasets composed primarily of diverse web text and specific domains such as mathematics and code. The training and validation sets have different distributions, requiring the evaluated models to demonstrate strong generalization capabilities. Our models incorporate RMSNorm (Zhang & Sennrich, 2019) for pre-normalization, ALiBi (Press et al., 2021) positional encoding for multi-head attention, and the SwiGLU (Shazeer,

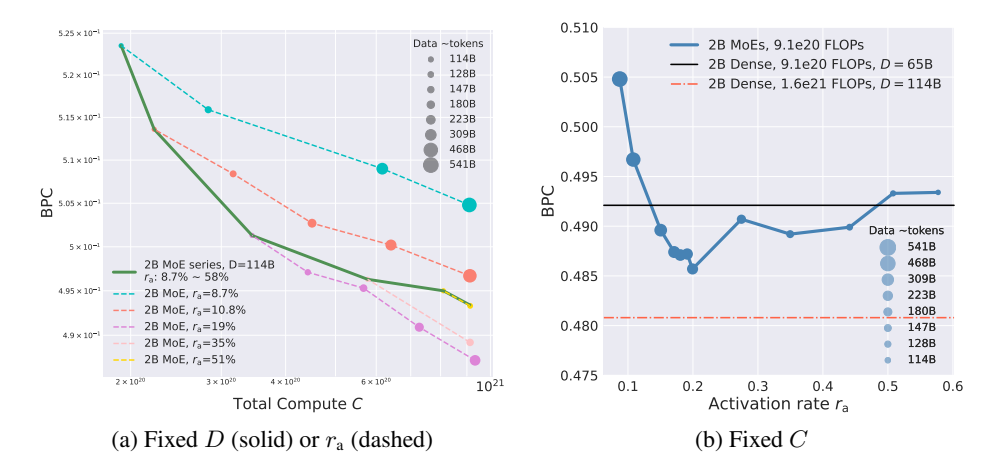


Figure 1: Performance of  $N \approx 2B$  models trained with varying data sizes D and activation rates  $r_a$ . (a) With a fixed D, performance gain exhibits a **non-linear** dependence on training budget C. Conversely, with a fixed  $r_a$ , increasing D leads to a **linear** performance gain. These findings indicate an optimal activation rate,  $r_a^{**} = 20\%$ , that is consistent across various D values when N is constant. (b) With a fixed training compute C, the optimal activation rate  $r_a^{**} = 20\%$  can be clearly seen.

2020) activation function for both feed-forward networks (FFNs) and MoE experts. The training procedures used consistently across all experiments are outlined in Table 3 in Appendix D. We employ cross-entropy loss ( $\mathcal{L}$ ) as the training metric and bits-per-character (BPC) as the validation metric.

## 4 OPTIMIZED MOE ARCHITECTURE

Building on the insights discussed above, we systematically examine the following model components in the order outlined below: 1) Distribution of MoE and dense layers. 2) Gate score normalization. 3) Parameter allocation within MoE. 4) Exploration of optimal structural hyperparameters. Each component incorporates previous conclusions into its experimental settings.

**MoE** and dense layers arrangement. This part examines how to arrange the distribution between MoE and dense layers. We consider three layer arrangement schemes: every layer is an MoE layer (full), one dense layer followed by MoE layers (ldense), and interleaved MoE and dense layers (interleave). We additionally include shared experts (SE) for some of our experiments.

Table 4 in Appendix D presents the experimental settings and results. The conclusions are as follows: 1) 1 dense+SE performs the best, possibly because the dense layer contributes to more stable training. 2) The ratio of shared expert size to total expert size  $D_{se}/(D_{se}+KD_{e})$  has minimal impact on model performance. Therefore, we continue using the 1 dense+SE configuration and set  $D_{se}=KD_{e}$ .

**Gate score normalization.** The results of normalizing gate scores of chosen experts are in Table 5 in Appendix D. Although the addition of normalization does not show an obvious difference in performance loss, it tends to reduce the average balance loss  $\bar{\mathcal{L}}_{\text{balance}}$ . Since normalization requires K > 1 to avoid zero gradient, we opt not to normalize given that some of our experiments have K=1.

**Top-K setting.** In this part, we discuss the allocation of parameters within MoE layers, focusing on the top-K setting. Expert granularity is adjusted by varying K and  $D_{\rm e}$  while keeping their product constant. We conduct three groups of experiments with various  $r_{\rm a}$  and the results are given in Table 6 in Appendix D. Note that within each experiment group, the product  $K \cdot D_{\rm e}$  is not strictly maintained due to compatibility with other hyperparameters. We observe that larger K generally hurts performance, except in the first group where K=1. We attribute this exception to the K=1 setting. Therefore, we prevent using large K and setting K=1 whenever possible.

**Model shape ratios.** As discussed in § 3.2, the shape hyperparameters include three ratios:  $\zeta$ ,  $\alpha$ , and  $\beta$ . We set  $\alpha=2.77$  (Touvron et al., 2023b) and explore the optimal  $\zeta$  and  $\mu$ , from which  $\beta$  can be derived. As illustrated in Fig. 4 in Appendix D, although performance fluctuates wildly given a

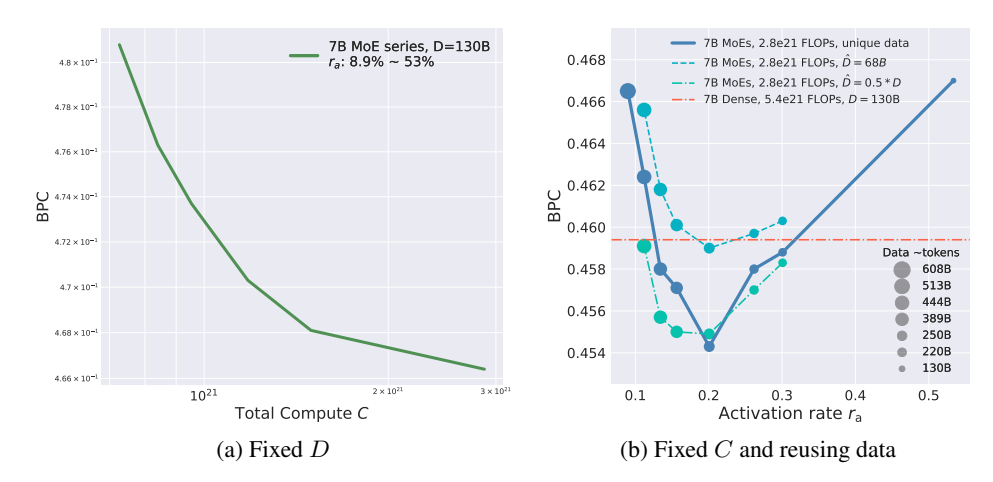


Figure 2: Performance of  $N \approx 7 B$  models trained with varying data sizes D and activation rate  $r_{\rm a}$ . The optimal activation rate,  $r_{\rm a}^{**}=20\%$ , align with the findings for the 2B models (Figure 1). Additionally, compared to training on the unique dataset, the strict data reuse scheme shows only a slight performance reduction, while the loose scheme often yields better performance.

value of  $\zeta$  or  $\mu$ , there is an overall upward trend with increasing  $D_{\rm m}$  for  $\zeta$  and a downward trend for  $\mu$ . Following the observed trend, we set  $\zeta \approx 88$  and  $\mu \approx 22$  for the subsequent experiments.

## 5 OPTIMAL ACTIVATION RATE

In this section, we analyze how the performance of MoE LLMs varies with different activation rates (AR) using model backbones optimized based on the conclusions in § 4, and examine whether MoE models can outperform dense models. Note that a concurrent study (Abnar et al., 2025) suggests that the optimal sparsity of MoE depends on model capacity. However, our findings indicate that, with optimized backbones, the optimal AR remains **consistent** across models of different sizes. We first detail our experimental setup and results, followed by a further discussion on the conclusions.

**Setup.** We built a series of MoE models with non-vocabulary parameters  $N \approx 2$ B and  $N \approx 7$ B, but varying activation rates  $r_a$  from 8.7% to 58%. Noteworthy, the model backbones were built upon the findings in § 4, as detailed in Table 8, 9, 10 and 11 in Appendix D. Each model was trained on a proportional subset of our dataset, ensuring  $D/N \ge 20$  (Hoffmann et al., 2022) for sufficient training.

## 5.1 OPTIMAL AR POINT

Focusing on the 2B models trained on the same data size D=114B as shown by the green solid line in Figure 1a, we observe that the performance gain **depends non-linearly** on the training budget C. Specifically, the gain is more significant within a relatively low range of  $r_{\rm a}$ . Starting from points on this curve and fixing the corresponding  $r_{\rm a}$  values, increasing D results in **linearly diminishing** BPC, as indicated by the dashed lines in Figure 1a. These results confirm the **existence of an optimal AR point**,  $r_{\rm a}^{**}$ , **that remains consistent regardless of** D **when** N **is unchanged**. When plotting the results from a fixed training compute perspective ( $C=C_0=9.1\rm{e}20$ ) in Figure 1b, we clearly observe that the optimal AR point is approximately  $r_{\rm a}^{**}\approx 20\%$ .

#### 5.2 Comparison with Dense Models

To compare with dense models, we trained two dense models (Table 12 in Appendix D) with  $N\approx 2$ B parameters and training budgets  $C_1=C_0=9.1$ e20 and  $C_2=1.64$ e21  $\approx 2C_1$ . The second model  $(C_2)$  is included for comparison to account for the typically lower Model FLOPs Utilization (MFU) in MoE training. This reduced MFU arises from load balancing and expert parallelism mechanisms that limit large-block matrix computations. As illustrated in Figure 1b, MoE models outperform their  $C_1$  dense counterparts when  $r_a$  falls within a specific range (approximately 15% to 48% for 2B models). For instance, the MoE model with the optimal AR point  $r_a^{**}=20\%$  achieves a BPC

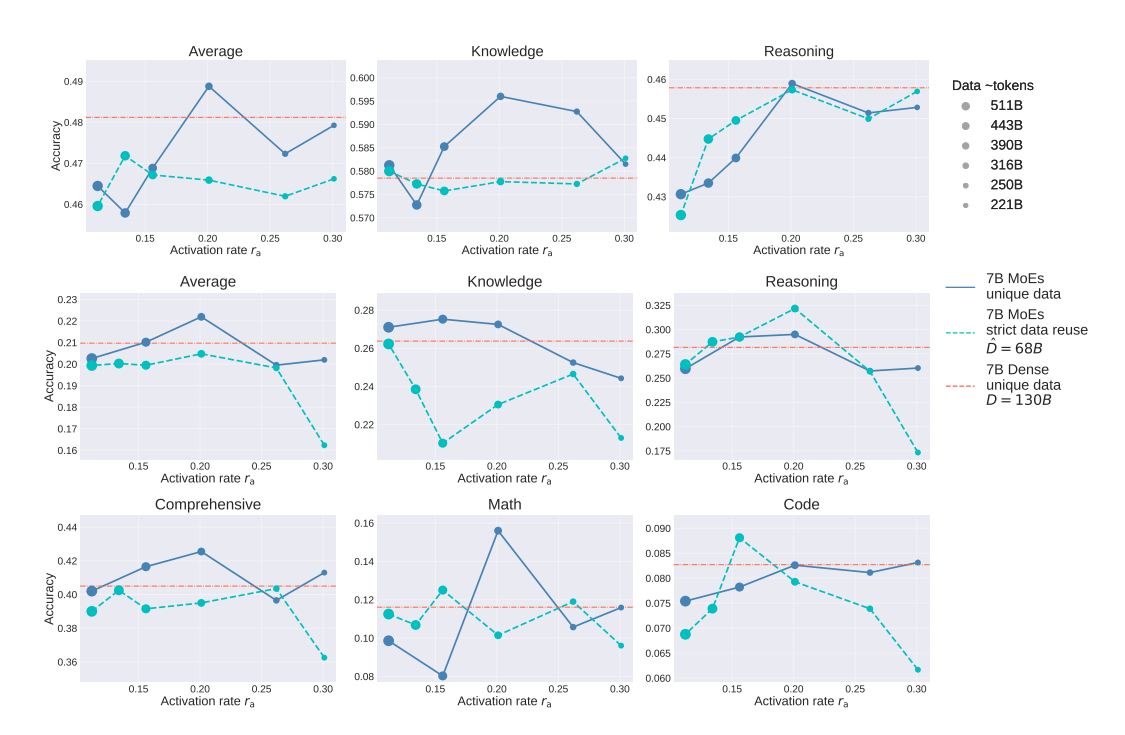


Figure 3: Downstream performance of 7B models: pre-trained (top) and SFT-ed (middle and bottom) versions. Across all benchmark types, MoE models with  $r_a = 20\%$  outperform dense model trained with twice the compute, aligning with upstream observations that the optimal AR is 20%.

value that is 0.0064 lower than its  $C_1$  dense counterpart and only 0.0049 higher than the  $C_2$  dense model. This demonstrates the existence of an *optimal activation rate region*  $R_{\rm a}^*$ , where **MoE models with**  $r_{\rm a} \in R_{\rm a}^*$  can outperform their dense counterparts under the same training budget C and approach the performance of dense models with double the compute. However, the performance gains of MoE models rely on a substantial increase in data, *e.g.*, a  $4.6 \times$  larger data size at  $r_{\rm a} = r_{\rm a}^{**} = 20\%$ . To mitigate this additional data requirement, we explore a data reuse strategy in § 6.

#### 5.3 Consistency of Optimal AR

As illustrated in Fig. 2, an optimal AR point  $r_{\rm a}^{**}$  also exists for 7B models. Surprisingly,  $r_{\rm a}^{**}$  remains consistent for both 2B and 7B models at approximately 20%, suggesting that  $r_{\rm a}^{**}$  is independent of model size. This finding contradicts established studies on MoE sparsity (Abnar et al., 2025), which proposes that optimal sparsity (defined as (E-K)/E) is directly proportional to model size. Nevertheless, our experiments were conducted with strictly controlled variables using optimized backbones, leading us to believe that our conclusions are both reliable and scalable (see Appendix B for a more detailed discussion). To further validate the possible universality of our findings, we conducted experiments on  $N \approx 3$ B models and achieved similar results (see Fig. 5 in Appendix D).

Expert specialization is another significant potential of MoEs in addition to remarkable scalability, where each expert focuses on learning specific features or patterns within the data. However, this attribute has not yet been clearly observed even in state-of-the-art MoE LLMs (Lo et al., 2024; Zhang et al., 2024), and effective approaches to achieve it remain under-explored. Based on our observation that MoEs outperform dense models when  $r_a \in R_a^*$ , we conjecture a relationship between the optimal AR region and the degree of expert specialization. Specifically: 1) When the activation rate is too low ( $r_a < 10\%$ ), the model lacks sufficient parameters to store knowledge effectively. 2) When the activation rate is relatively high ( $r_a > 50\%$ ), more experts are typically activated, which may lead to weaker specialization. An activation rate within the optimal region  $R_a^*$  likely facilitates a higher degree of expert specialization, thereby enhancing the MoE model's performance compared to its dense counterpart. We leave further analysis of this potential relationship for future work.

378 379

Table 2: Accuracy of 7B SFT-ed models across different benchmarks.

380
381
382
383
384
385
386
387
388
389
390
391
392

Dense baseline MoE w/ optimal AR Activation rate 20.07 20.07 Pretrain info Compute 5.45e21 2.86e21 2.86e21 Data reuse strict CMMLU (Li et al., 2023) 31.23 31.62 32.11 MMLU (Hendrycks et al., 2020) 31.26 32.92 24.57 Knowledge MMLU-Redux (Gema et al., 2024) 28 90 30.93 23 73 MMLU-Pro (Wang et al., 2024) 14.12 13.59 13.59 DROP (Dua et al., 2019) 32.32 35.13 30.93 Reasoning LiveBench (White et al., 2024) 16.82 18.15 16.76 MUSR (Sprague et al., 2023) 35.98 35.58 48.94 21.02 AGIEval (Zhong et al., 2023) 20.89 22.07 Comprehensive BBH (Suzgun et al., 2022) 58.02 60.01 56.07 GAOKAO-Math24 (Zhang et al., 2023) 9.92 15.70 9.09 Math GSM8K (Cobbe et al., 2021) 13.34 15.54 11.22 APPS (Hendrycks et al., 2021) 7.35 6.80 8.18 DS-1000 (Lai et al., 2023) 5.70 6.90 4.60 Code HumanEval (Chen et al., 2021) 22.56 21.34 21.95 1.67 LeetCode (Coignion et al., 2024) 1.49 1.49 LiveCodeBench (Jain et al., 2024) 4.21 3.37 4.63

396 397

399 400 401

402 403

404 405

406

407

408

409

410

411

412

413

414

415

416 417

418

419

420

421

422

423

424

425 426

428

429

430

431

394

## 6 Data Reuse Strategy

As discussed in § 5.2, MoEs outperform their dense counterparts but require additional data. To eliminate this increased data demand, we investigate data reusability by training models for multiple epochs using a fixed, smaller dataset size  $\hat{D}$ . We extract a sub-dataset of size  $\hat{D}$  from the original training dataset. At the beginning of each epoch after the first, the data are shuffled.

**Setup.** We explore two distinct schemes, termed the *strict* and the *loose* data reuse schemes.

For the strict scheme, our aim is to ensure that both MoE and dense models are trained under completely equal conditions with respect to N, D, and C. Given a fixed  $\hat{D}$ , the number of training epochs (ranging from 1.7 to 8.3 in our 3B and 7B model experiments) increases as  $r_{\rm a}$  decreases (hence decreasing M) to maintain the compute budget C. The experimental settings are detailed in Table 13, 14, 15, in Appendix D, which are mostly the same as those in § 5.2, except for the training data used. Specifically, we set  $\hat{D}=65{\rm B}$  and 114B for the 3B models, and  $\hat{D}=68{\rm B}$  for the 7B models, corresponding to the data used for training the dense models.

For the loose scheme, we relax the constraint of identical D by fixing the number of training epochs to 2 for all  $r_a$ , hence  $\hat{D}=0.5D$ , where the exact value of D corresponds to the specific  $r_a$ . We conduct experiments on 7B models and the experimental settings are in Table 16 in Appendix D.

**Results.** The performance under the strict scheme is illustrated by the blue dashed lines in Fig. 2b and 5 in Appendix D. Reusing data  $\hat{D}$  only marginally diminishes performance compared to training on the unique dataset D for a single epoch, and MoE models continue to outperform dense baselines. Moreover, increasing  $\hat{D}$  further narrows the performance gap. The similarity in curve shapes indicates that the optimal activation rate  $r_a^{**}$  remains unchanged. These findings address the primary question posed at the beginning of this paper: **Mixture-of-Experts can surpass dense LLMs under equal total parameters, compute, and data constraints, provided that the backbones are optimized and r\_a \in R\_a^\*. Surprisingly, the loose scheme (green dashed line) often outperforms training with unique dataset. Similar results are observed on certain downstream tasks (§ 7).** 

**Discussion.** Prior works have explored the effectiveness of multi-epoch training for dense and MoE models. Muennighoff et al. (2023) developed a scaling law that accounts for the number of repeated tokens and found negligible loss for repeating up to 4 epochs compared to training on unique data, whereas Hernandez et al. (2022) showed degradation for dense models. Xue et al. (2023) noticed no significant gain for MoEs with repeated training when high-quality data is insufficient. Here we performed multi-epoch training on partial subsets of the unique dataset under the optimal AR setting, and found that 2-epoch data reuse boosts MoE performance over unique data, and the performance

degradation is minimal when the number of epochs further increases. We hypothesize that MoE routers benefit from additional epochs, potentially leading to more refined routing decisions and thereby mitigate the negative impact observed in dense models.

## 7 ANALYSIS OF DOWNSTREAM PERFORMANCE

To assess whether the optimal ARs generalize to downstream tasks, we conduct SFT on our 7B pre-trained models (trained w/ and w/o strict data reuse) and evaluate both the pre-trained models and SFT-ed models on a total number of 29 benchmarks (see Fig. 3 and Tab. 2), including categories such as reasoning and knowledge. The comprehensive list of benchmarks can be found in Appendix C. For all SFT trainings, we use a fixed data size D, and thus varying C across models with different  $r_a$ . The 7B dense model trained with twice the compute is included for comparison.

MoE vs. Dense at  $r_a = r_a^{**}$ . For both PT and SFT models, MoEs outperform their dense equivalents across all benchmark types when  $r_a = 20\%$ . This result aligns with upstream findings that the optimal activation rate  $(r_a^{**})$  is 20%, highlighting the very possible universality of the optimal AR point across different training phases and data domains. Furthermore,  $r_a^{**}$  remains unchanged during SFT, even with varying C, suggesting that the SFT data size may have an upper limit for performance improvement, provided the PT model is adequately trained. Additionally, the <code>average</code> performance at  $r_a \neq r_a^{**}$  is consistently inferior to that of dense models, underscoring the critical role of the optimal AR point.

**MoE** vs. Dense at  $r_a < r_a^{**}$ . Dense models outperform MoEs across all domains for PT models. After SFT, MoEs overtake dense models on comprehensive and knowledge tasks. However, a notable performance gap remains in math, highlighting the PT stage's importance for math ability.

 **MoE** vs. Dense at  $r_{\rm a} > r_{\rm a}^{**}$ . Compared to the dense models, MoEs perform better on knowledge but worse on reasoning for PT models, and usually slightly underperform after SFT.

 **Sparser** vs. **Denser.** For PT models, denser MoEs  $(r_a > r_a^{**})$  outperform or match the performance of sparser MoEs  $(r_a < r_a^{**})$  across all domains, consistent with Figure 2b, regardless of data reuse. When training on unique data, sparser MoEs perform better on knowledge. Notably, denser MoE performance significantly degrades with data reuse, especially for SFT.

**Impact of data reuse.** For both PT and SFT models, data reuse has little impact on reasoning but causes significant degradation in knowledge performance. Surprisingly, at  $r_a = r_a^{**}$ , the SFT-ed MoEs trained with data reuse outperform both MoEs and dense models trained on unique data. This implies that a model can master reasoning skills (rather than merely memorizing information (Hu et al., 2024)) with a relatively small dataset (Muennighoff et al., 2025; Wang et al., 2025) and further enhance its capabilities through multiple training epochs.

#### 8 CONCLUSION AND FUTURE WORKS

In this paper, we propose a three-step experimental methodology to investigate whether MoEs can surpass their dense counterparts under the same constraints on total parameters, compute, and data. By optimizing the architecture, identifying the optimal activation rate region, and reusing data, we arrive at a positive answer to this question. Future work will explore how optimal activation rates enhance model capabilities and whether similar conclusions hold for other training methods like upcycling (Komatsuzaki et al., 2022) and MoEfication (Zhang et al., 2021). We hope this work offers valuable insights for the architectural design of next-generation models.

### LIMITATIONS

The limitations of this work include: 1) Hindering by the high computational cost, we did not train models larger than 7B. 2) As described in § 4, we focus mainly on the impact of several main components of MoEs, but fix the rest to narrow the scale of experiments. 3) Exploration of other elements can provide further comprehensive guidance for the architectural design of MoEs.

## REFERENCES

- Samira Abnar, Harshay Shah, Dan Busbridge, Alaaeldin Mohamed Elnouby Ali, Josh Susskind, and Vimal Thilak. Parameters vs flops: Scaling laws for optimal sparsity for mixture-of-experts language models. *arXiv preprint arXiv:2501.12370*, 2025.
- Josh Achiam, Steven Adler, Sandhini Agarwal, Lama Ahmad, Ilge Akkaya, Florencia Leoni Aleman, Diogo Almeida, Janko Altenschmidt, Sam Altman, Shyamal Anadkat, et al. Gpt-4 technical report. arXiv preprint arXiv:2303.08774, 2023.
- Jinze Bai, Shuai Bai, Yunfei Chu, Zeyu Cui, Kai Dang, Xiaodong Deng, Yang Fan, Wenbin Ge, Yu Han, Fei Huang, et al. Qwen technical report. *arXiv preprint arXiv:2309.16609*, 2023.
- Yonatan Bisk, Rowan Zellers, J Gao, and Y Choi. Piqa: reasoning about physical commonsense in natural language. corr, vol. abs/1911.11641, 2019.
- Mark Chen, Jerry Tworek, Heewoo Jun, Qiming Yuan, Henrique Ponde De Oliveira Pinto, Jared Kaplan, Harri Edwards, Yuri Burda, Nicholas Joseph, Greg Brockman, et al. Evaluating large language models trained on code. *arXiv preprint arXiv:2107.03374*, 2021.
- Christopher Clark, Kenton Lee, Ming-Wei Chang, Tom Kwiatkowski, Michael Collins, and Kristina Toutanova. Boolq: Exploring the surprising difficulty of natural yes/no questions. *arXiv* preprint *arXiv*:1905.10044, 2019.
- Peter Clark, Isaac Cowhey, Oren Etzioni, Tushar Khot, Ashish Sabharwal, Carissa Schoenick, and Oyvind Tafjord. Think you have solved question answering? try arc, the ai2 reasoning challenge. *arXiv preprint arXiv:1803.05457*, 2018.
- Karl Cobbe, Vineet Kosaraju, Mohammad Bavarian, Mark Chen, Heewoo Jun, Lukasz Kaiser, Matthias Plappert, Jerry Tworek, Jacob Hilton, Reiichiro Nakano, et al. Training verifiers to solve math word problems. *arXiv preprint arXiv:2110.14168*, 2021.
- Tristan Coignion, Clément Quinton, and Romain Rouvoy. A performance study of llm-generated code on leetcode. In *Proceedings of the 28th International Conference on Evaluation and Assessment in Software Engineering*, pp. 79–89, 2024.
- Damai Dai, Chengqi Deng, Chenggang Zhao, RX Xu, Huazuo Gao, Deli Chen, Jiashi Li, Wangding Zeng, Xingkai Yu, Y Wu, et al. Deepseekmoe: Towards ultimate expert specialization in mixture-of-experts language models. *arXiv preprint arXiv:2401.06066*, 2024.
- DeepSeek-AI, :, Xiao Bi, Deli Chen, Guanting Chen, Shanhuang Chen, Damai Dai, and et al. Deepseek llm: Scaling open-source language models with longtermism, 2024a. URL https://arxiv.org/abs/2401.02954.
- DeepSeek-AI, Aixin Liu, Bei Feng, Bing Xue, Bingxuan Wang, Bochao Wu, and etc. Deepseek-v3 technical report, 2024b. URL https://arxiv.org/abs/2412.19437.
- Dheeru Dua, Yizhong Wang, Pradeep Dasigi, Gabriel Stanovsky, Sameer Singh, and Matt Gardner. Drop: A reading comprehension benchmark requiring discrete reasoning over paragraphs. *arXiv* preprint arXiv:1903.00161, 2019.
- William Fedus, Barret Zoph, and Noam Shazeer. Switch transformers: Scaling to trillion parameter models with simple and efficient sparsity. *Journal of Machine Learning Research*, 23(120):1–39, 2022.
- Aryo Pradipta Gema, Joshua Ong Jun Leang, Giwon Hong, Alessio Devoto, Alberto Carlo Maria Mancino, Rohit Saxena, Xuanli He, Yu Zhao, Xiaotang Du, Mohammad Reza Ghasemi Madani, et al. Are we done with mmlu? *arXiv preprint arXiv:2406.04127*, 2024.
- Ethan He, Abhinav Khattar, Ryan Prenger, Vijay Korthikanti, Zijie Yan, Tong Liu, Shiqing Fan, Ashwath Aithal, Mohammad Shoeybi, and Bryan Catanzaro. Upcycling large language models into mixture of experts. *arXiv preprint arXiv:2410.07524*, 2024.

- Dan Hendrycks, Collin Burns, Steven Basart, Andy Zou, Mantas Mazeika, Dawn Song, and Jacob Steinhardt. Measuring massive multitask language understanding. *arXiv preprint arXiv:2009.03300*, 2020.
  - Dan Hendrycks, Steven Basart, Saurav Kadavath, Mantas Mazeika, Akul Arora, Ethan Guo, Collin Burns, Samir Puranik, Horace He, Dawn Song, et al. Measuring coding challenge competence with apps. *arXiv preprint arXiv:2105.09938*, 2021.
  - Danny Hernandez, Tom Brown, Tom Conerly, Nova DasSarma, Dawn Drain, Sheer El-Showk, Nelson Elhage, Zac Hatfield-Dodds, Tom Henighan, Tristan Hume, Scott Johnston, Ben Mann, Chris Olah, Catherine Olsson, Dario Amodei, Nicholas Joseph, Jared Kaplan, and Sam McCandlish. Scaling laws and interpretability of learning from repeated data, 2022. URL https://arxiv.org/abs/2205.10487.
  - Jordan Hoffmann, Sebastian Borgeaud, Arthur Mensch, Elena Buchatskaya, Trevor Cai, Eliza Rutherford, Diego de Las Casas, Lisa Anne Hendricks, Johannes Welbl, Aidan Clark, et al. Training compute-optimal large language models. *arXiv preprint arXiv:2203.15556*, 2022.
  - Junjie Hu, Sebastian Ruder, Aditya Siddhant, Graham Neubig, Orhan Firat, and Melvin Johnson. Xtreme: A massively multilingual multi-task benchmark for evaluating cross-lingual generalisation. In *International conference on machine learning*, pp. 4411–4421. PMLR, 2020.
  - Yi Hu, Xiaojuan Tang, Haotong Yang, and Muhan Zhang. Case-based or rule-based: How do transformers do the math? In *Forty-first International Conference on Machine Learning, ICML 2024, Vienna, Austria, July 21-27, 2024*. OpenReview.net, 2024. URL https://openreview.net/forum?id=4Vqr8SRfyX.
  - Naman Jain, King Han, Alex Gu, Wen-Ding Li, Fanjia Yan, Tianjun Zhang, Sida Wang, Armando Solar-Lezama, Koushik Sen, and Ion Stoica. Livecodebench: Holistic and contamination free evaluation of large language models for code. *arXiv preprint arXiv:2403.07974*, 2024.
  - Albert Q Jiang, Alexandre Sablayrolles, Antoine Roux, Arthur Mensch, Blanche Savary, Chris Bamford, Devendra Singh Chaplot, Diego de las Casas, Emma Bou Hanna, Florian Bressand, et al. Mixtral of experts. *arXiv preprint arXiv:2401.04088*, 2024.
  - Jared Kaplan, McCandlish Sam, Henighan Tom, T.B. Brown, Chess Benjamin, Rewon Child, Scott Gray, Alec Radford, Jeffrey Wu, and Dario Amodei. Scaling laws for neural language models. *arXiv: Learning, arXiv: Learning*, Jan 2020.
  - Aran Komatsuzaki, Joan Puigcerver, James Lee-Thorp, Carlos Riquelme Ruiz, Basil Mustafa, Joshua Ainslie, Yi Tay, Mostafa Dehghani, and Neil Houlsby. Sparse upcycling: Training mixture-of-experts from dense checkpoints. *arXiv preprint arXiv:2212.05055*, 2022.
  - Tom Kwiatkowski, Jennimaria Palomaki, Olivia Redfield, Michael Collins, Ankur Parikh, Chris Alberti, Danielle Epstein, Illia Polosukhin, Matthew Kelcey, Jacob Devlin, Kenton Lee, Kristina N. Toutanova, Llion Jones, Ming-Wei Chang, Andrew Dai, Jakob Uszkoreit, Quoc Le, and Slav Petrov. Natural questions: a benchmark for question answering research. *Transactions of the Association of Computational Linguistics*, 2019.
  - Guokun Lai, Qizhe Xie, Hanxiao Liu, Yiming Yang, and Eduard Hovy. RACE: Large-scale ReAding comprehension dataset from examinations. In Martha Palmer, Rebecca Hwa, and Sebastian Riedel (eds.), *Proceedings of the 2017 Conference on Empirical Methods in Natural Language Processing*, pp. 785–794, Copenhagen, Denmark, September 2017. Association for Computational Linguistics. doi: 10.18653/v1/D17-1082. URL https://aclanthology.org/D17-1082/.
  - Yuhang Lai, Chengxi Li, Yiming Wang, Tianyi Zhang, Ruiqi Zhong, Luke Zettlemoyer, Wen-tau Yih, Daniel Fried, Sida Wang, and Tao Yu. Ds-1000: A natural and reliable benchmark for data science code generation. In *International Conference on Machine Learning*, pp. 18319–18345. PMLR, 2023.
  - Dmitry Lepikhin, HyoukJoong Lee, Yuanzhong Xu, Dehao Chen, Orhan Firat, Yanping Huang, Maxim Krikun, Noam Shazeer, and Zhifeng Chen. Gshard: Scaling giant models with conditional computation and automatic sharding. *arXiv* preprint arXiv:2006.16668, 2020.

- Haonan Li, Yixuan Zhang, Fajri Koto, Yifei Yang, Hai Zhao, Yeyun Gong, Nan Duan, and Timothy
   Baldwin. Cmmlu: Measuring massive multitask language understanding in chinese. arXiv preprint
   arXiv:2306.09212, 2023.
  - Houyi Li, Wenzhen Zheng, Jingcheng Hu, Qiufeng Wang, Hanshan Zhang, Zili Wang, Shijie Xuyang, Yuantao Fan, Shuigeng Zhou, Xiangyu Zhang, et al. Predictable scale: Part i–optimal hyperparameter scaling law in large language model pretraining. *arXiv preprint arXiv:2503.04715*, 2025.
  - Ka Man Lo, Zeyu Huang, Zihan Qiu, Zili Wang, and Jie Fu. A closer look into mixture-of-experts in large language models. *arXiv preprint arXiv:2406.18219*, 2024.
  - Jan Ludziejewski, Maciej Pióro, Jakub Krajewski, Maciej Stefaniak, Michał Krutul, Jan Małaśnicki, Marek Cygan, Piotr Sankowski, Kamil Adamczewski, Piotr Miłoś, and Sebastian Jaszczur. Joint moe scaling laws: Mixture of experts can be memory efficient, 2025. URL https://arxiv.org/abs/2502.05172.
  - Niklas Muennighoff, Alexander Rush, Boaz Barak, Teven Le Scao, Nouamane Tazi, Aleksandra Piktus, Sampo Pyysalo, Thomas Wolf, and Colin A Raffel. Scaling data-constrained language models. *Advances in Neural Information Processing Systems*, 36:50358–50376, 2023.
  - Niklas Muennighoff, Zitong Yang, Weijia Shi, Xiang Lisa Li, Li Fei-Fei, Hannaneh Hajishirzi, Luke Zettlemoyer, Percy Liang, Emmanuel Candès, and Tatsunori Hashimoto. s1: Simple test-time scaling. *arXiv preprint arXiv:2501.19393*, 2025.
  - Ofir Press, Noah A Smith, and Mike Lewis. Train short, test long: Attention with linear biases enables input length extrapolation. *arXiv preprint arXiv:2108.12409*, 2021.
  - Qwen, :, An Yang, Baosong Yang, Beichen Zhang, Binyuan Hui, Bo Zheng, and et al. Qwen2.5 technical report, 2025. URL https://arxiv.org/abs/2412.15115.
  - Alec Radford. Improving language understanding by generative pre-training. 2018.
  - Samyam Rajbhandari, Conglong Li, Zhewei Yao, Minjia Zhang, Reza Yazdani Aminabadi, Ammar Ahmad Awan, Jeff Rasley, and Yuxiong He. Deepspeed-moe: Advancing mixture-of-experts inference and training to power next-generation ai scale, 2022. URL https://arxiv.org/abs/2201.05596.
  - Keisuke Sakaguchi, Ronan Le Bras, Chandra Bhagavatula, and Yejin Choi. Winogrande: An adversarial winograd schema challenge at scale. *Communications of the ACM*, 64(9):99–106, 2021.
  - Maarten Sap, Hannah Rashkin, Derek Chen, Ronan LeBras, and Yejin Choi. Socialiqa: Commonsense reasoning about social interactions. *arXiv preprint arXiv:1904.09728*, 2019.
  - Noam Shazeer. Glu variants improve transformer. arXiv preprint arXiv:2002.05202, 2020.
  - Noam Shazeer, Azalia Mirhoseini, Krzysztof Maziarz, Andy Davis, Quoc Le, Geoffrey Hinton, and Jeff Dean. Outrageously large neural networks: The sparsely-gated mixture-of-experts layer. *arXiv* preprint arXiv:1701.06538, 2017.
  - Zayne Sprague, Xi Ye, Kaj Bostrom, Swarat Chaudhuri, and Greg Durrett. Musr: Testing the limits of chain-of-thought with multistep soft reasoning. *arXiv* preprint arXiv:2310.16049, 2023.
  - Mirac Suzgun, Nathan Scales, Nathanael Schärli, Sebastian Gehrmann, Yi Tay, Hyung Won Chung, Aakanksha Chowdhery, Quoc V Le, Ed H Chi, Denny Zhou, et al. Challenging big-bench tasks and whether chain-of-thought can solve them. *arXiv preprint arXiv:2210.09261*, 2022.
  - Hugo Touvron, Thibaut Lavril, Gautier Izacard, Xavier Martinet, Marie-Anne Lachaux, Timothée Lacroix, Baptiste Rozière, Naman Goyal, Eric Hambro, Faisal Azhar, et al. Llama: Open and efficient foundation language models. *arXiv preprint arXiv:2302.13971*, 2023a.
  - Hugo Touvron, Louis Martin, Kevin Stone, Peter Albert, Amjad Almahairi, Yasmine Babaei, Nikolay Bashlykov, Soumya Batra, Prajjwal Bhargava, Shruti Bhosale, et al. Llama 2: Open foundation and fine-tuned chat models. *arXiv preprint arXiv:2307.09288*, 2023b.

- A Vaswani. Attention is all you need. Advances in Neural Information Processing Systems, 2017.
  - Yiping Wang, Qing Yang, Zhiyuan Zeng, Liliang Ren, Lucas Liu, Baolin Peng, Hao Cheng, Xuehai He, Kuan Wang, Jianfeng Gao, et al. Reinforcement learning for reasoning in large language models with one training example. *arXiv* preprint arXiv:2504.20571, 2025.
  - Yubo Wang, Xueguang Ma, Ge Zhang, Yuansheng Ni, Abhranil Chandra, Shiguang Guo, Weiming Ren, Aaran Arulraj, Xuan He, Ziyan Jiang, et al. Mmlu-pro: A more robust and challenging multitask language understanding benchmark. In *The Thirty-eight Conference on Neural Information Processing Systems Datasets and Benchmarks Track*, 2024.
  - Tianwen Wei, Bo Zhu, Liang Zhao, Cheng Cheng, Biye Li, Weiwei Lü, Peng Cheng, Jianhao Zhang, Xiaoyu Zhang, Liang Zeng, et al. Skywork-moe: A deep dive into training techniques for mixture-of-experts language models. *arXiv preprint arXiv:2406.06563*, 2024.
  - Johannes Welbl, Nelson F Liu, and Matt Gardner. Crowdsourcing multiple choice science questions. *arXiv preprint arXiv:1707.06209*, 2017.
  - Colin White, Samuel Dooley, Manley Roberts, Arka Pal, Ben Feuer, Siddhartha Jain, Ravid Shwartz-Ziv, Neel Jain, Khalid Saifullah, Siddartha Naidu, et al. Livebench: A challenging, contamination-free llm benchmark. *arXiv preprint arXiv:2406.19314*, 2024.
  - Shaohua Wu, Jiangang Luo, Xi Chen, Lingjun Li, Xudong Zhao, Tong Yu, Chao Wang, Yue Wang, Fei Wang, Weixu Qiao, et al. Yuan 2.0-m32: Mixture of experts with attention router. *arXiv* preprint arXiv:2405.17976, 2024.
  - Liang Xu, Hai Hu, Xuanwei Zhang, Lu Li, Chenjie Cao, Yudong Li, Yechen Xu, Kai Sun, Dian Yu, Cong Yu, et al. Clue: A chinese language understanding evaluation benchmark. *arXiv preprint arXiv:2004.05986*, 2020.
  - Fuzhao Xue, Yao Fu, Wangchunshu Zhou, Zangwei Zheng, and Yang You. To repeat or not to repeat: Insights from scaling Ilm under token-crisis, 2023. URL https://arxiv.org/abs/2305.13230.
  - Fuzhao Xue, Zian Zheng, Yao Fu, Jinjie Ni, Zangwei Zheng, Wangchunshu Zhou, and Yang You. Openmoe: An early effort on open mixture-of-experts language models. *arXiv preprint* arXiv:2402.01739, 2024.
  - An Yang, Baosong Yang, Binyuan Hui, Bo Zheng, Bowen Yu, Chang Zhou, Chengpeng Li, Chengyuan Li, Dayiheng Liu, Fei Huang, Guanting Dong, Haoran Wei, Huan Lin, Jialong Tang, Jialin Wang, Jian Yang, Jianhong Tu, Jianwei Zhang, Jianxin Ma, Jianxin Yang, Jin Xu, Jingren Zhou, Jinze Bai, Jinzheng He, Junyang Lin, Kai Dang, Keming Lu, Keqin Chen, Kexin Yang, Mei Li, Mingfeng Xue, Na Ni, Pei Zhang, Peng Wang, Ru Peng, Rui Men, Ruize Gao, Runji Lin, Shijie Wang, Shuai Bai, Sinan Tan, Tianhang Zhu, Tianhao Li, Tianyu Liu, Wenbin Ge, Xiaodong Deng, Xiaohuan Zhou, Xingzhang Ren, Xinyu Zhang, Xipin Wei, Xuancheng Ren, Xuejing Liu, Yang Fan, Yang Yao, Yichang Zhang, Yu Wan, Yunfei Chu, Yuqiong Liu, Zeyu Cui, Zhenru Zhang, Zhifang Guo, and Zhihao Fan. Qwen2 technical report, 2024. URL https://arxiv.org/abs/2407.10671.
  - Rowan Zellers, Ari Holtzman, Yonatan Bisk, Ali Farhadi, and Yejin Choi. Hellaswag: Can a machine really finish your sentence? *arXiv preprint arXiv:1905.07830*, 2019.
  - Biao Zhang and Rico Sennrich. Root mean square layer normalization. *Advances in Neural Information Processing Systems*, 32, 2019.
  - Xiaotian Zhang, Chunyang Li, Yi Zong, Zhengyu Ying, Liang He, and Xipeng Qiu. Evaluating the performance of large language models on gaokao benchmark. *arXiv preprint arXiv:2305.12474*, 2023.
  - Zeliang Zhang, Xiaodong Liu, Hao Cheng, Chenliang Xu, and Jianfeng Gao. Diversifying the expert knowledge for task-agnostic pruning in sparse mixture-of-experts. *arXiv* preprint *arXiv*:2407.09590, 2024.

Zhengyan Zhang, Yankai Lin, Zhiyuan Liu, Peng Li, Maosong Sun, and Jie Zhou. Moefication: Transformer feed-forward layers are mixtures of experts. *arXiv preprint arXiv:2110.01786*, 2021.

Wanjun Zhong, Ruixiang Cui, Yiduo Guo, Yaobo Liang, Shuai Lu, Yanlin Wang, Amin Saied, Weizhu Chen, and Nan Duan. Agieval: A human-centric benchmark for evaluating foundation models. arXiv preprint arXiv:2304.06364, 2023.

Barret Zoph, Irwan Bello, Sameer Kumar, Nan Du, Yanping Huang, Jeff Dean, Noam Shazeer, and William Fedus. St-moe: Designing stable and transferable sparse expert models. *arXiv* preprint arXiv:2202.08906, 2022.

## **APPENDIX**

## A BACKGROUND: MIXTURE-OF-EXPERTS

The MoE architecture primarily consists of a gate and several experts. Typically, the gate  $g(\cdot)$  is composed of a linear layer  $W_g$  followed by a Softmax and a Top-K operation, and the experts  $E_{i=1,...N}$  follow the standard FFN structure. The computation of an MoE block can then be formulated as follows:

$$y = \sum_{i=1}^{N} g_i(x) \cdot E_i(x),$$
(11)

$$g_i(x) = \begin{cases} s_i & \text{if } s_i \in \text{TopK}(s; K), \\ 0 & \text{otherwise,} \end{cases}$$
 (12)

where  $s_i = \text{Softmax}_i(W_g x)$  denotes the gate score for the *i*-th expert.

# B EXTENDED ANALYSIS ON RELATED WORK

We notice a concurrent work (Abnar et al., 2025) studied scaling law for optimal MoE sparsity. We highlight the differences between our work and theirs as follows:

- **Formulation**: We define "sparsity" as the activation rate  $r_a = N_a/N$ , which is a more general definition than that proposed by Abnar et al. (2025), namely the ratio of inactive experts to the total number of experts, (E K)/E.
- **Methodology**: Given that the activation rate  $r_a$  does not depend on the underlying model architecture, we can thus easily take into consideration other components such as shared expert and build all our models upon the optimized architecture proposed in § 4. This ensures the observed performance differences solely attribute to the varying activation rates.
- Experiments: Our 2B and 7B models utilized approximately  $9 \times$  and  $30 \times$  more compute than their (larger) models to ensure a sufficiently large D/N ratio. Consequently, their conclusions are likely based on undertrained models.
- **Conclusion**: We discover an optimal activation rate that appears to be *independent* of model sizes, whereas Abnar et al. (2025) find that the optimal sparsity increases with model size.

Our conclusion regarding a consistent optimal activation rate contradicts the findings of Abnar et al. (2025). While we believe our findings are reliable, given that our experiments are conducted with strictly controlled variables using *optimized backbones* and *sufficient training data*, we acknowledge the possibility that the optimal  $r_a$  might slightly shift for model sizes significantly beyond our studied range (i.e., N >> 7B). Nevertheless, we contend that the optimal  $r_a$  can be considered consistent within a certain range of model sizes, in contrast to the significant changes reported by Abnar et al. (2025).

# C COMPREHENSIVE LIST OF BENCHMARKS

To assess whether the optimal ARs generalize to downstream tasks, we conduct SFT on our 7B pre-trained models (trained w/ and w/o strict data reuse) and evaluate both the pre-trained models and SFT-ed models on a total number of 29 benchmarks (Figure 3). The comprehensive list of benchmarks is provided here.

For pre-trained models, we evaluate on:

- Knowledge: BBH (Suzgun et al., 2022), PIQA (Bisk et al., 2019), SCIQ (Welbl et al., 2017), SIQA (Sap et al., 2019)
- Reasoning: ARC (Clark et al., 2018), BoolQ (Clark et al., 2019), CLUE (Xu et al., 2020), DROP (Dua et al., 2019), HellaSwag (Zellers et al., 2019), NaturalQA (Kwiatkowski et al., 2019), RACE (Lai et al., 2017), WinoGrande (Sakaguchi et al., 2021), XTREME (Hu et al., 2020)

For SFT-ed models, we evaluate on:

- Comprehensive: AGIEVAL (Zhong et al., 2023), BBH
- Knowledge: CMMLU (Li et al., 2023), MMLU (Hendrycks et al., 2020), MMLU-Redux (Gema et al., 2024), MMLU-Pro (Wang et al., 2024)
- Reasoning: DROP, LiveBench (White et al., 2024), MuSR (Sprague et al., 2023)
- Math: GAOKAO-Math24 (Zhang et al., 2023), GSM8K (Cobbe et al., 2021)
- Code: APPS (Hendrycks et al., 2021), DS-1000 (Lai et al., 2023), HumanEval (Chen et al., 2021), LeetCode (Coignion et al., 2024), LiveCodeBench (Jain et al., 2024)

# D MORE EXPERIMENTAL RESULTS

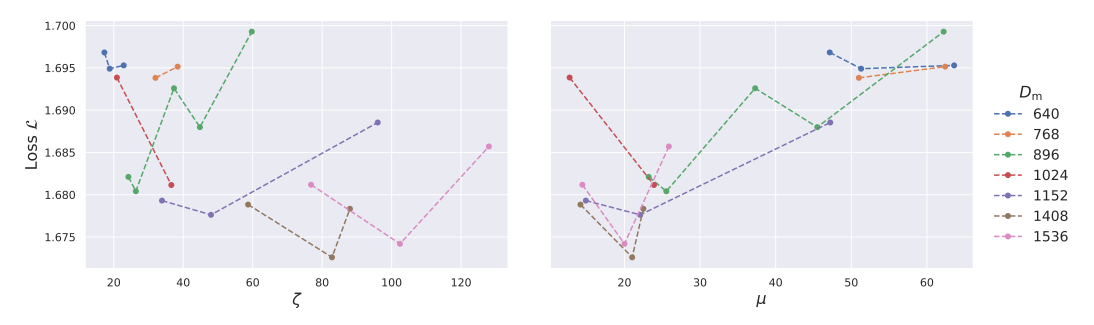


Figure 4: Results for model shape ratios  $\zeta$  and  $\mu$ . An overall upward trend is observed in  $\zeta$  as  $D_{\rm m}$  increases, while  $\mu$  exhibits a downward trend with increasing  $D_{\rm m}$ .

Table 3: Common training recipe.

Hyperparameter	Setting
Vocab	65536
Optimizer	Adam
Weight decay	0.1
Gradient clipping norm	1.0
LR Scheduler	Cosine
Warmup iters	$clip(0.01 \cdot Iters, 200, 2000)$
Min LR	1e-5

Table 4: Experimental settings and results of MoE layer arrangement and shared expert. Hyperparameters shared by all experiments:  $D_{\rm m}=1408, D_{\rm ffn}=3904, {\rm Norm}={\rm True}.$ 

N	$N_{\rm a}$	M	H	$D_{h}$	L	E	K	$D_{\mathrm{e}}$	$D_{se}$	Scheme	$\mathcal{L}$	Conclusion
2.02B 2.02B 2.02B	346M 346M 346M	8.77e8 8.77e8 8.77e8	22 22 22	64 64 64	16 16 16	35 68 70	2 2 4	800 800 800	1600 1600 0	full+SE interleave+SE interleave	1.6813 1.6766 1.6697	interleave performs better than full
2.15B	366M	6.63e9	11	128	16	85	5	352	1760	1dense+SE	1.8700	1dense+SE performs the best
2.15B	366M	6.63e9	22	64	16	85	5	352	1760	1dense+SE	1.8557	
2.15B	367M	6.63e9	11	128	16	70	4	800	0	interleave	1.8737	
2.15B	367M	6.63e9	22	64	16	70	4	800	0	interleave	1.8620	
2.15B	368M	9.31e8	22	64	17	37	4	800	0	1dense	1.6752	$rac{D_{ m se}}{(D_{ m se}+KD_{ m e})}$ impacts little
2.15B	368M	9.31e8	22	64	17	36	3	800	800	1dense+SE	1.6712	
2.15B	368M	9.31e8	22	64	17	35	2	800	1600	1dense+SE	1.6726	

Table 5: Experimental settings and results of gate score normalization. Hyperparameters shared by all experiments: Scheme = 1 dense, L=17,  $D_{\rm m}=1408$ ,  $D_{\rm ffn}=3904$ , H=22,  $D_{\rm h}=64$ .

$\overline{N}$	$N_{\rm a}$	r <sub>a</sub> (%)	M	E	K	$D_{\mathrm{e}}$	$D_{se}$	Norm	L	$\bar{\mathcal{L}}_{balance}$
2.15B 2.15B	368M 368M	17.08 17.08	9.31e8 9.31e8	35 35	2 2	800 800	1600 1600	Y N	1.6726 1.6712	<b>1.355</b> 1.452
2.15B 2.15B	368M 368M	17.08 17.08	9.31e8 9.31e8	37 37	4 4	800 800	0	Y N	1.6752 1.6750	<b>1.409</b> 1.440

## E THE USE OF LARGE LANGUAGE MODELS: AN EXPLANATION

Only a small fraction of complex paragraphs are written with the assistance and modification of ChatGPT. For instance, we provide the prompt: "I am writing an academic conference paper in the field of computer science. Please help me polish the wording of this paragraph, organize the sentences, and express them in a more academic way." After that the outputs are rigorously reviewed to ensure accuracy and appropriateness.

Table 6: Experimental settings and results of top-K setting. Hyperparameters shared by all experiments: Scheme =  $1 \text{dense}, L = 16, D_{\text{m}} = 1408, D_{\text{ffn}} = 3904, H = 11, D_{\text{h}} = 128, \text{Norm} = \text{False}$ .

N	$N_{\rm a}$	$r_{\rm a}~(\%)$	M	E	K	$D_{\mathrm{e}}$	$D_{se}$	$\mathcal{L}$
2.15B	591M	27.47	8.00e9	8	1	3528	3528	2.0470
2.15B	591M	27.40	8.00e9	88	11	320	3520	<b>2.0338</b>
2.15B	949M	44.00	1.01e10	8	2	3176	6352	<b>1.9996</b> 2.0266
2.15B	948M	44.05	1.01e10	88	22	288	6336	
2.15B	1.24B	57.57	1.19e10	8	3	2888	8664	<b>2.0156</b> 2.0235
2.11B	1.22B	57.68	1.18e10	88	33	256	8448	

Table 7: Experimental settings and results of model shape ratios. Hyperparameters shared by all experiments: Scheme = 1 dense, S = 16384,  $D_{\rm h} = 128$ .

N	$N_{\mathrm{a}}$	$D_{\mathrm{m}}$	$D_{ m ffn}$	L	Н	E	K	$D_{e}$	$D_{se}$	$\mu$	ζ	$\mathcal{L}$
2.15e9	3.67e8	640	1774	34	5	50	4	608	2432	51.30	20.39	1.694
2.15e9	3.69e8	640	1774	37	5	38	3	736	2208	47.15	18.78	1.696
2.14e9	3.69e8	640	1774	49	5	41	3	512	1536	35.20	14.33	1.695
2.14e9	3.67e8	768	2129	20	6	99	8	448	3584	62.42	41.42	1.693
2.15e9	3.69e8	896	2484	15	7	124	10	416	4160	62.21	65.00	1.699
2.15e9	3.68e8	896	2484	20	7	91	7	416	2912	45.50	48.16	1.687
2.13e9	3.67e8	896	2484	24	7	54	4	576	2304	37.29	39.96	1.692
2.15e9	3.69e8	896	2484	34	7	61	4	352	1408	25.54	28.15	1.680
2.16e9	3.68e8	896	2484	37	7	47	3	416	1248	23.21	25.89	1.682
2.14e9	3.70e8	1024	2839	28	8	80	5	288	1440	23.91	38.93	1.681
2.16e9	3.69e8	1024	2839	49	8	49	2	256	512	12.75	22.33	1.693
2.15e9	3.67e8	1152	3194	12	9	79	6	640	3840	47.22	105.73	1.688
2.14e9	3.68e8	1152	3194	34	9	64	3	256	768	14.89	35.91	1.679
2.15e9	3.69e8	1280	3549	28	10	113	5	160	800	14.75	48.41	1.675
2.15e9	3.70e8	1408	3904	24	11	46	2	416	832	14.18	62.22	1.678
2.13e9	3.68e8	1536	4258	12	12	65	4	576	2304	25.88	140.64	1.685
2.16e9	3.68e8	1536	4258	15	12	91	5	320	1600	20.00	110.71	1.674
2.15e9	3.66e8	1536	4258	20	12	95	4	224	896	14.44	81.84	1.681
2.16e9	3.68e8	1792	4968	15	14	128	5	192	960	14.25	129.00	1.693
2.14e9	3.67e8	1920	5323	12	15	71	3	416	1248	16.03	175.55	1.699

Table 8: Experimental settings and results of optimal ARs for MoE models with N=2.15B and fixed  $r_{\rm a}$ . Hyperparameters shared by all experiments:  $L=16, S=2048, D_{\rm m}=1408, D_{\rm ffn}=3904, H=11, D_{\rm h}=128, \zeta=88.$ 

$N_{\mathrm{a}}$	r <sub>a</sub> (%)	M	D	C	D/N	E	K	$D_{\mathrm{e}}$	$D_{se}$	η	В	# Iters	BPC
1.88e8	8.74	1.68e9	1.14e11	1.92e20	53	89	1	352	352	2.01e-3	672	82833	0.5235
1.88e8	8.74	1.68e9	1.68e11	2.83e20	78	89	1	352	352	2.26e-3	832	98771	0.5159
1.88e8	8.74	1.68e9	3.67e11	6.16e20	170	89	1	352	352	2.87e-3	1344	133187	0.5090
1.88e8	8.74	1.68e9	5.41e11	9.10e20	252	89	1	352	352	3.24e-3	1728	152927	0.5048
2.33e8	10.81	1.95e9	1.14e11	2.22e20	53	88	2	352	704	2.01e-3	672	82833	0.5136
2.33e8	10.81	1.95e9	1.62e11	3.16e20	75	88	2	352	704	2.24e-3	896	88446	0.5084
2.33e8	10.81	1.95e9	2.31e11	4.50e20	107	88	2	352	704	2.49e-3	1024	110149	0.5027
2.33e8	10.81	1.95e9	3.29e11	6.41e20	153	88	2	352	704	2.78e-3	1280	125427	0.5002
2.33e8	10.81	1.95e9	4.68e11	9.12e20	218	88	2	352	704	3.10e-3	1600	142822	0.4967
4.11e8	19.11	3.02e9	1.14e11	3.44e20	53	84	6	352	2112	2.01e-3	672	82833	0.5013
4.11e8	19.11	3.02e9	1.46e11	4.42e20	68	84	6	352	2112	2.17e-3	768	93015	0.4971
4.11e8	19.11	3.02e9	1.88e11	5.67e20	87	84	6	352	2112	2.34e-3	960	95469	0.4953
4.11e8	19.11	3.02e9	2.41e11	7.27e20	112	84	6	352	2112	2.52e-3	1024	114870	0.4909
4.11e8	19.11	3.02e9	3.09e11	9.34e20	144	84	6	352	2112	2.73e-3	1280	117950	0.4872
7.52e8	34.95	5.06e9	1.14e11	5.77e20	53	84	15	320	4800	2.01e-3	672	82833	0.4963
7.52e8	34.95	5.06e9	1.80e11	9.13e20	84	84	15	320	4800	2.31e-3	896	98256	0.4892
1.09e9	50.79	7.11e9	1.14e11	8.10e20	53	84	26	288	7488	2.01e-3	672	82833	0.4950
1.09e9	50.79	7.11e9	1.28e11	9.13e20	60	84	26	288	7488	2.08e-3	704	89125	0.4933

Table 9: Experimental settings and results of optimal ARs for MoE models N=2.15B with fixed C. Hyperparameters shared by all experiments:  $L=16, S=2048, D_{\rm m}=1408, D_{\rm ffn}=3904, H=11, D_{\rm h}=128, \zeta=88$ . The green row corresponds to the MoE model with the lowest BPC on the validation set.

$N_{\mathrm{a}}$	$r_{\rm a}(\%)$	M	D	C	D/N	$\mu$	E	K	$D_{\mathrm{e}}$	$D_{\mathrm{se}}$	$\eta$	B	# Iters	BPC
1.88e8	8.74	1.70e9	5.41e11	9.18e20	252	22.50	89	1	352	352	3.24e-3	1728	152927	0.5048
2.33e8	10.82	1.96e9	4.68e11	9.19e20	218	22.50	88	2	352	704	3.10e-3	1600	142822	0.4967
3.24e8	15.04	2.50e9	3.75e11	9.38e20	174	22.50	86	4	352	1408	2.89e-3	1344	136378	0.4896
3.68e8	17.11	2.77e9	3.39e11	9.38e20	158	22.50	85	5	352	1760	2.80e-3	1296	127756	0.4874
3.89e8	18.06	2.89e9	3.25e11	9.38e20	151	22.50	93	6	320	1920	2.76e-3	1280	123862	0.4871
4.11e8	19.12	3.03e9	3.09e11	9.38e20	144	22.50	84	6	352	2112	2.73e-3	1280	117950	0.4872
4.29e8	19.94	3.13e9	2.99e11	9.38e20	139	22.50	92	7	320	2240	2.70e-3	1248	117177	0.4857
5.90e8	27.46	4.10e9	2.23e11	9.15e20	104	22.55	8	1	3528	3528	2.46e-3	1024	106335	0.4907
7.52e8	34.96	5.08e9	1.80e11	9.16e20	84	22.50	84	15	320	4800	2.31e-3	896	98256	0.4892
9.48e8	44.11	6.25e9	1.47e11	9.16e20	68	22.56	8	2	3176	6352	2.16e-3	768	93460	0.4899
1.09e9	50.80	7.12e9	1.29e11	9.15e20	60	22.50	84	26	288	7488	2.08e-3	704	89125	0.4933
1.24e9	57.73	8.01e9	1.14e11	9.13e20	53	22.56	8	3	2888	8664	2.006e-3	672	82833	0.4934

Table 10: Experimental settings and results of optimal ARs for MoE models with N=6.52B with fixed D. Hyperparameters shared by all experiments:  $L=24, S=2048, D_{\rm m}=2048, D_{\rm ffn}=5464, H=16, D_{\rm h}=128, \zeta=85.3$ .

$N_{\mathrm{a}}$	r <sub>a</sub> (%)	M	D	C	D/N	E	K	$D_{\mathrm{e}}$	$D_{se}$	η	В	# Iters	BPC
7.26e8	11.15	5.59e9	1.30e11	7.25e20	19.90	82	2	512	1024	4.74e-4	640	98816	0.4808
8.70e8	13.36	6.46e9	1.30e11	8.37e20	19.90	81	3	512	1536	4.74e-4	640	98816	0.4763
1.02e9	15.67	7.33e9	1.30e11	9.49e20	19.90	80	4	512	2048	4.74e-4	640	98816	0.4737
1.31e9	20.03	9.07e9	1.30e11	1.17e21	19.88	78	6	512	3072	4.74e-4	640	98816	0.4703
1.70e9	26.11	1.15e10	1.30e11	1.48e21	19.90	86	10	448	4480	4.74e-4	640	98816	0.4681
3.47e9	53.30	2.21e10	1.30e11	2.86e21	19.90	84	28	384	10752	4.74e-4	640	98816	0.4664

Table 11: Experimental settings and results of optimal ARs for MoE models with N=6.52B with fixed C. Hyperparameters shared by all experiments:  $L=24, S=2048, D_{\rm m}=2048, D_{\rm ffn}=5464, H=16, D_{\rm h}=128, \zeta=85.3$ . The green row corresponds to the MoE model with the lowest BPC on the validation set.

$N_a$	$r_{\rm a}(\%)$	M	D	C	D/N	μ	E	K	$D_{\rm e}$	$D_{\rm se}$	η	В	# Iters	BPC
5 05 20	8.97	4.73e9	6.05.11	2.86e21	02.88	21.00	02	1	512	512	7.620.4	1512	195502	0.4665
5.85e8			6.05e11		92.88		83	1	512	512	7.62e-4	1512		
7.30e8	11.19	5.59e9	5.11e11	2.86e21	78.47	21.00	82	2	512	1024	7.23e-4	1360	183630	0.4624
8.74e8	13.41	6.46e9	4.43e11	2.86e21	67.93	21.00	81	3	512	1536	6.92e-4	1232	175482	0.4580
1.02e9	15.63	7.33e9	3.90e11	2.86e21	59.89	21.00	80	4	512	2048	6.64e-4	1152	165447	0.4571
1.31e9	20.07	9.07e9	3.16e11	2.86e21	48.50	21.00	78	6	512	3072	6.23e-4	1040	148410	0.4543
1.71e9	26.18	1.15e10	2.50e11	2.86e21	38.32	21.00	86	10	448	4480	5.80e-4	960	127035	0.4580
1.96e9	30.07	1.30e10	2.21e11	2.86e21	33.83	21.00	84	12	448	5376	5.57e-4	800	134597	0.4588
3.48e9	53.38	2.21e10	1.30e11	2.86e21	19.87	21.00	84	28	384	10752	4.74e-4	640	98816	0.4670

Table 12: Experimental settings and results of optimal ARs for 2B, 3B, and 7B dense baselines.

$\overline{}$	M	D	C	D/N	L	Н	$D_{m}$	$D_{ m ffn}$	η	В	# Iters	BPC
2.15e9	1.44e10	6.50e10	9.36e20	30.23	28	17	2176	8848	8.44e-4	320	99182	0.4921
2.15e9	1.44e10	1.14e11	1.64e21	53.02	28	17	2176	8848	1.00e-3	448	124032	0.4808
3.29e9	2.24e10	6.26e10	1.40e21	19.03	44	19	2432	7008	1.23e-3	448	68253	0.4833
3.29e9	2.24e10	1.25e11	2.80e21	38.06	44	19	2432	7008	1.52e-3	640	95554	0.4684
6.48e9	4.21e10	6.80e10	2.86e21	10.49	32	32	4096	11008	3.89e-4	432	76813	0.4736
6.48e9	4.21e10	1.30e11	5.45e21	20.00	32	32	4096	11008	4.76e-4	640	98816	0.4594

Table 13: Experimental settings and results of data reusing ( $\hat{D}=68\mathrm{B}$ ) for MoE models with  $N=6.52\mathrm{B}$  with fixed C. Hyperparameters shared by all experiments:  $L=24, S=2048, D_\mathrm{m}=2048, D_\mathrm{fin}=5464, H=16, D_\mathrm{h}=128, \zeta=85.3$ . The green row corresponds to the MoE model with the lowest BPC on the validation set.

$N_{\mathrm{a}}$	$r_{\rm a}(\%)$	M	D	Epoch	M	D/N	μ	E	K	$D_{\mathrm{e}}$	$D_{se}$	η	В	# Iters	BPC
7.30e8	11.19	5.59e9	5.11e11	7.52	2.86e21	78.47	21.00	82	2	512	1024	7.23e-4	1344	185816	0.4656
8.74e8	13.41	6.46e9	4.43e11	6.51	2.86e21	67.93	21.00	81	3	512	1536	6.92e-4	1232	175482	0.4618
1.02e9	15.63	7.33e9	3.90e11	5.74	2.86e21	59.89	21.00	80	4	512	2048	6.64e-4	1152	165447	0.4601
1.31e9	20.07	9.07e9	3.16e11	4.65	2.86e21	48.50	21.00	78	6	512	3072	6.23e-4	1024	150729	0.4590
1.71e9	26.18	1.15e10	2.50e11	3.67	2.86e21	38.32	21.00	86	10	448	4480	5.80e-4	960	127035	0.4597
1.96e9	30.07	1.30e10	2.21e11	3.24	2.86e21	33.83	21.00	84	12	448	5376	5.57e-4	792	135956	0.4603

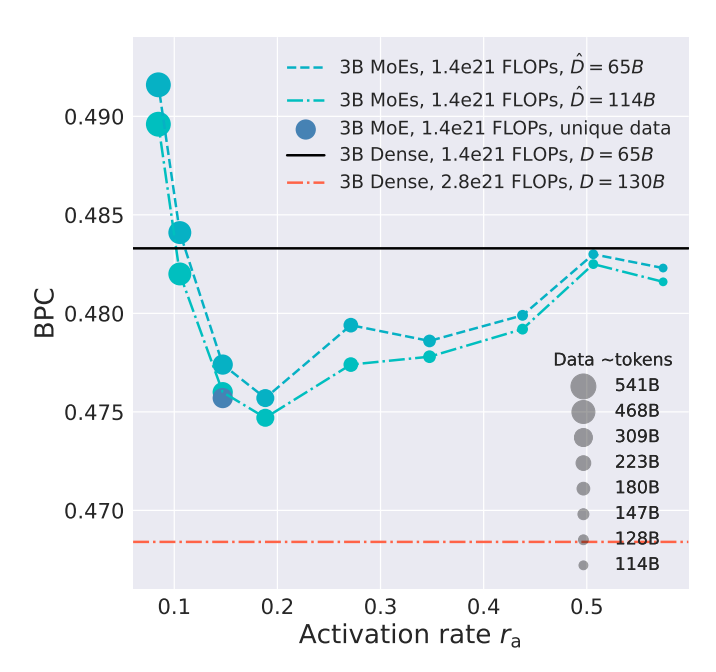


Figure 5: Performance of  $N \approx 3$ B models trained with varying data sizes D and activation rate  $r_{\rm a}$ . The optimal activation rate,  $r_{\rm a}^{**}=20\%$ , aligns with the findings for the 2B models (Figure 1). Additionally, compared to training on the unique dataset, the data reuse scheme shows only a slight performance reduction. To save computational costs, only one model trained on unique data is included for reference.

Table 14: Experimental settings and results of strict data reuse ( $\ddot{D}=65\mathrm{B}$ ) for MoE models with  $N=3.29\mathrm{B}$  with fixed C. Hyperparameters shared by all experiments:  $L=24, S=2048, D_\mathrm{m}=1408, D_\mathrm{ffn}=3904, H=11, D_\mathrm{h}=128$ . The green row corresponds to the MoE model with the lowest BPC on the validation set.

$N_{\rm a}$	$r_{\rm a}(\%)$	D	Epoch	M	C	D/N	E	K	$D_{\mathrm{e}}$	$D_{se}$	η	В	# Iters	BPC
2.78e8	8.46	5.41e11	8.33	2.51e9	1.36e21	164.62	89	1	352	352	3.24e-3	1728	152927	0.4916
3.47e8	10.54	4.68e11	7.20	2.92e9	1.36e21	142.36	88	2	352	704	3.10e-3	1600	142822	0.4841
4.83e8	14.70	3.75e11	5.78	3.74e9	1.40e21	114.19	86	4	352	1408	2.89e-3	1344	136378	0.4774
6.20e8	18.83	3.09e11	4.76	4.56e9	1.41e21	94.06	84	6	352	2112	2.73e-3	1280	117950	0.4757
8.93e8	27.12	2.23e11	3.43	6.19e9	1.38e21	67.74	8	1	3528	3528	2.465e-3	1024	106335	0.4794
1.14e9	34.75	1.80e11	2.77	7.69e9	1.39e21	54.85	84	15	320	4800	2.31e-3	896	98256	0.4786
1.44e9	43.77	1.47e11	2.26	9.48e9	1.39e21	44.52	8	2	3176	6352	2.169e-3	768	93460	0.4799
1.66e9	50.63	1.29e11	1.98	1.08e10	1.39e21	39.09	84	26	288	7488	2.08e-3	704	89125	0.4830
1.89e9	57.40	1.14e11	1.75	1.22e10	1.39e21	34.61	8	3	2888	8664	2.006e-3	672	82833	0.4823

Table 15: Experimental settings and results of data reuse ( $\hat{D}=114\mathrm{B}$ ) for MoE models with  $N=3.29\mathrm{B}$  with fixed C. Hyperparameters shared by all experiments:  $L=24, S=2048, D_{\mathrm{m}}=1408, D_{\mathrm{ffn}}=3904, H=11, D_{\mathrm{h}}=128$ . The green row corresponds to the MoE model with the lowest BPC on the validation set.

$N_{\mathrm{a}}$	$r_{\mathrm{a}}(\%)$	D	Epoch	M	C	D/N	E	K	$D_{\mathrm{e}}$	$D_{se}$	$\eta$	B	# Iters	BPC
2.78e8	8.46	5.41e11	4.75	2.51e9	1.36e21	164.62	89	1	352	352	3.24e-3	1728	152927	0.4896
3.47e8	10.54	4.68e11	4.11	2.92e9	1.36e21	142.36	88	2	352	704	3.10e-3	1600	142822	0.4820
4.83e8	14.70	3.75e11	3.29	3.74e9	1.40e21	114.19	86	4	352	1408	2.89e-3	1344	136378	0.4760
6.20e8	18.83	3.09e11	2.71	4.56e9	1.41e21	93.93	84	6	352	2112	2.73e-3	1280	117950	0.4747
8.93e8	27.12	2.23e11	1.96	6.19e9	1.38e21	67.74	8	1	3528	3528	2.465e-3	1024	106335	0.4774
1.14e9	34.75	1.80e11	1.58	7.69e9	1.39e21	54.85	84	15	320	4800	2.31e-3	896	98256	0.4778
1.44e9	43.77	1.47e11	1.29	9.48e9	1.39e21	44.52	8	2	3176	6352	2.169e-3	768	93460	0.4792
1.66e9	50.63	1.29e11	1.13	1.08e10	1.39e21	39.09	84	26	288	7488	2.08e-3	720	87144	0.4825
1.89e9	57.40	1.14e11	1.00	1.22e10	1.39e21	34.61	8	3	2888	8664	2.006e-3	672	82833	0.4816

Table 16: Experimental settings and results of loose data reuse for MoE models with  $N=6.52\mathrm{B}$  with fixed C. Hyperparameters shared by all experiments:  $L=24, S=2048, D_{\mathrm{m}}=2048, D_{\mathrm{ffn}}=5464, H=16, D_{\mathrm{h}}=128$ . The green row corresponds to the MoE model with the lowest BPC on the validation set.

$N_{\rm a}$	$r_{\rm a}(\%)$	ĥ	M	C	D/N	E	K	$D_{e}$	$D_{se}$	η	В	# Iters	BPC
7.30e8	11.19	2.56e11	5.59e9	2.86e21	78.47	82	2	512	1024	7.23e-4	1344	185816	0.4591
8.74e8	13.41	2.21e11	6.46e9	2.86e21	67.93	81	3	512	1536	6.92e-4	1232	175482	0.4557
1.02e9	15.63	1.95e11	7.33e9	2.86e21	59.89	80	4	512	2048	6.64e-4	1152	165447	0.4550
1.31e9	20.07	1.58e11	9.07e9	2.87e21	48.50	78	6	512	3072	6.23e-4	1024	150729	0.4549
1.71e9	26.18	1.25e11	1.15e10	2.86e21	38.32	86	10	448	4480	5.80e-4	960	127035	0.4570
1.96e9	30.07	1.10e11	1.30e10	2.86e21	33.83	84	12	448	5376	5.57e-4	792	135956	0.4583